Impact of ethanol on the flotation efficiency of imidazolium ionic liquids as collectors: Insights from dynamic surface tension and solvation analysis

Qian Cheng, Zerui Lei, Guangjun Mei, and Jianhua Chen

Articles you may be interested in

Tao Wei, Qi Zhang, Sijia Wang, Mengting Wang, Ye Liu, Cheng Sun, Yanyan Zhou, Qing Huang, Xiangyun Qiu, and Fang Tian, A gel polymer electrolyte with IL@UiO-66-NH$_2$ as fillers for high-performance all-solid-state lithium metal batteries, *Int. J. Miner. Metall. Mater.*, 30(2023), No. 10, pp. 1897-1905. https://doi.org/10.1007/s12613-023-2639-0

Zhengde Pang, Yuyang Jiang, Jiawei Ling, Xuewei Lü, and Zhiming Yan, Blast furnace ironmaking process with super high TiO$_2$ in the slag: Density and surface tension of the slag, *Int. J. Miner. Metall. Mater.*, 29(2022), No. 6, pp. 1170-1178. https://doi.org/10.1007/s12613-021-2262-x

Fei Cao, Wei Wang, De-zhou Wei, and Wen-gang Liu, Separation of tungsten and molybdenum with solvent extraction using functionalized ionic liquid tricaprylmethylammonium bis(2,4,4-trimethylpentyl)phosphinate, *Int. J. Miner. Metall. Mater.*, 28(2021), No. 11, pp. 1769-1776. https://doi.org/10.1007/s12613-020-2172-3

Qicheng Feng, Wanming Lu, Han Wang, and Qian Zhang, Mechanistic insights into stepwise activation of malachite for enhancing surface reactivity and flotation performance, *Int. J. Miner. Metall. Mater.*, 31(2024), No. 10, pp. 2159-2172. https://doi.org/10.1007/s12613-023-2793-4

Jon Derek Loftis and Tarek M. Abdel-Fattah, Nanoscale electropolishing of high-purity nickel with an ionic liquid, *Int. J. Miner. Metall. Mater.*, 26(2019), No. 5, pp. 649-656. https://doi.org/10.1007/s12613-019-1773-1

Zhongxian Wu, Dongping Tao, Youjun Tao, Man Jiang, and Patrick Zhang, A novel cationic collector for silicon removal from collophane using reverse flotation under acidic conditions, *Int. J. Miner. Metall. Mater.*, 30(2023), No. 6, pp. 1038-1047. https://doi.org/10.1007/s12613-022-2580-7

IJMMM WeChat   QQ author group

Impact of ethanol on the flotation efficiency of imidazolium ionic liquids as collectors: Insights from dynamic surface tension and solvation analysis

Qian Cheng[1,2], *Zerui Lei*[1], *Guangjun Mei*[1,2,✉]*, and Jianhua Chen*[2]

1) Key Laboratory of Green Utilization of Critical Non-metallic Mineral Resources, Ministry of Education, Wuhan University of Technology, Wuhan 430070, China
2) MOE Key Laboratory of New Processing Technology for Non-ferrous Metals and Materials, Guangxi Key Laboratory of Processing for Non-ferrous Metals and Featured Materials, Guangxi University, Nanning 530004, China

Abstract: To conduct extensive research on the application of ionic liquids as collectors in mineral flotation, ethanol (EtOH) was used as a solvent to dissolve hydrophobic ionic liquids (ILs) to simplify the reagent regime. Interesting phenomena were observed in which EtOH exerted different effects on the flotation efficiency of two ILs with similar structures. When EtOH was used to dissolve 1-dodecyl-3-methylimidazolium chloride (C_{12}[mim]Cl) and as a collector for pure quartz flotation tests at a concentration of 1×10^{-5} mol·L^{-1}, quartz recovery increased from 23.77% to 77.91% compared with ILs dissolved in water. However, quartz recovery of 1-dodecyl-3-methylimidazolium hexafluorophosphate (C_{12}[mim]PF_6) decreased from 60.45% to 24.52% under the same conditions. The conditional experiments under 1×10^{-5} mol·L^{-1} ILs for EtOH concentration and under 2vol% EtOH for ILs concentration confirmed this difference. After being affected by EtOH, the mixed ore flotation tests of quartz and hematite showed a decrease in the hematite concentrate grade and recovery for the C_{12}[mim]Cl collector, whereas the hematite concentrate grade and recovery for the C_{12}[mim]PF_6 collector increased. On the basis of these differences and observations of flotation foam, two-phase bubble observation tests were carried out. The EtOH promoted the foam height of two ILs during aeration. It accelerated static froth defoaming after aeration stopped, and the foam of C_{12}[mim]PF_6 defoaming especially quickly. In the discussion of flotation tests and foam observation, an attempt was made to explain the reasons and mechanisms behind the diverse phenomena using the dynamic surface tension effect and solvation effect results from EtOH. The solvation effect was verified through Fourier transform infrared (FT-IR), X-ray photoelectron spectroscopy (XPS), and Zeta potential tests. Although EtOH affects the adsorption of ILs on the ore surface during flotation negatively, it holds an positive value of inhibiting foam merging during flotation aeration and accelerating the defoaming of static foam. And induce more robust secondary enrichment in the mixed ore flotation of the C_{12}[mim]PF_6 collector, facilitating effective mixed ore separation even under inhibitor-free conditions.

Keywords: ionic liquid; ethanol; flotation foam; solvation; dynamic surface tension

1. Introduction

Ionic liquids (ILs) are contemporary chemical agents developed within the framework of green chemistry. They are salts composed of organic cations and either inorganic or organic anions, with melting points below 100 or 150°C [1]. They evolved from traditional elevated-temperature molten salts but are quite different from conventional ionic compounds. The electrostatic attraction between anions and cations in ILs is weak, allowing them to have smaller lattice energies and exist in a liquid state at or near room temperature [2]. ILs possess unique and excellent chemical and thermodynamic stability, a wide liquid range, great solubility for organic and inorganic substances, good electrical conductivity, high ion mobility and diffusion speed, nonflammability, odorlessness, and other advantages [3–5]. As a new type of environmentally friendly liquid material with promising ap-

plications, the research and application of ILs have progressed rapidly [6–8]. A notable unique feature of ILs is their designability. The physical and chemical properties of ILs can be tuned and improved by using different combinations of anions and cations or by fine-tuning the alkyl chains of cations. They are called "green designable solvents" [9].

In the field of mineral flotation research, quartz is a commonly encountered gangue mineral. The use of amine collectors in reverse flotation to separate quartz from target minerals has become a viable option [10–12]. However, traditional amine collectors, such as dodecylamine and etheramine, have disadvantages such as high foam viscosity, challenging defoaming, and poor selectivity [13–14]. To enhance flotation performance, ongoing research has explored new cationic collectors [15–17]. In recent years, ILs with excellent chemical properties, environmental friendliness, and good controllability have been studied for application in flot-

🍃 Springer

2646

Int. J. Miner. Metall. Mater., Vol. 31, No. 12, Dec. 2024

ation. Certain ILs with strong collecting ability, good selectivity, and excellent flotation performance were screened and synthesized.

Li *et al*. [18] used a phosphonium-nitrogen-based ionic liquid for rare earth flotation and evaluated the [N_{2222}] [EHEHP] ionic liquid for REM flotation. They found that the [EHEHP] moiety can be adsorbed onto hematite and bastnasite, likely by chemisorption, with no clear evidence showing reagent adsorption on the quartz surface [18]. Azizi *et al*. [19] used tetrabutylammonium bis(2-ethylhexyl)-phosphate for rare earth flotation and monazite recovery; it was explored as a collector for the flotation of model monazite and bastnasite minerals of complex REE-bearing ores. They compared the selectivity and collecting power of this collector with those of conventional hydroxamic acid-containing collectors. Zhu *et al*. [20] prepared and synthesized IL microemulsion collector for coal flotation and studied the interfacial composition and thermodynamic parameters of [$C_n$mim]Cl (n = 12, 14, or 16)/n-alcohol (C_4–C_6)/n-dodecane/water microemulsion systems by using Schulman's titration. Qiu *et al*. [21] investigated different ILs in the flotation of $LiAlO_2$ and its gangue mineral melilite s.s. A significant influence of the hardness of the counter anions chloride and bromide of the ILs is observed during flotation. Sahoo *et al*. [22] used quaternary ammonium ionic liquid for flotation experiments. TOMAS, a newly synthesized quaternary ammonium salt ionic liquid with salicylic acid as a ligand, achieves promising results in the flotation separation of quartz and hematite [22]. The application of the three-carbon chain quaternary ammonium salt 336 in hematite beneficiation was studied [23], as well as the flotation behavior of the four-carbon chain quaternary ammonium salt influenced by the carbon chain [24]. A simple comparison was conducted between traditional flotation reagents, quaternary ammonium salts, imidazole, pyridine and other IL flotation [25]. Li *et al*. [26] studied quaternary ammonium salt-based ionic liquid collectors. Compared with tricaprylmethyl ammonium salicylate (TOMAS), lengthening the carbon chain enhances the collection performance and reduces the reagent dose, resulting in significantly better separation. Zhou *et al*. [27] studied the combination of tetradecyl dimethyl benzyl ammonium chloride and sodium isobutyl xanthate to prepare ILs, which were applied to the desiliconization and desulfurization of bauxite. Yuan *et al*. [28] synthesized sulfur-containing ionic liquids (SCILs) from quaternary ammonium cations and xanthate anions and applied them as collectors. They concluded that SCILs have excellent collecting ability and selectivity for pyrrhotite flotation against magnetite flotation compared with the traditional collector of sodium isobutyl xanthate (SIBX). Cheng *et al*. [29] used four types of imidazole ILs as collectors for the separation flotation of quartz and hematite.

ILs have better collector properties and selectivities than traditional amine collector dichlorodiphenyl-ducgloroethane (DDA) owing to the strong overall charge of ionic liquid adsorbent semimicelle, but the local charge is weak. Wu *et al*. [30] used ionic liquid 1-dodecyl-3-methylimidazolium chloride as a collector to recover Y_2O_3 from phosphors using flotation.

In this study, C_{12}[mim]Cl and C_{12}[mim]PF_6 were used as collectors, and the effect of ethanol (EtOH) on the flotation separation of quartz and hematite was investigated. For the first time, differences in the effects of ethanol on the flotation efficiency of C_{12}[mim]Cl and C_{12}[mim]PF_6 were discovered. At a specific concentration of ethanol, C_{12}[mim]PF_6 can achieve good separation efficiency in mixed flotation of quartz and hematite without using inhibitors. In addition, a certain concentration of ethanol can reduce foam merger during flotation and expedite defoaming after the foam is removed. This study analyzed the influence of ethanol on these phenomena through dynamic surface tension and the solvation effect. This research holds significant value in exploring the flotation rules of IL collectors, analyzing the flotation performance differences between hydrophilic and hydrophobic ILs, and promoting the application of ethanol as an adjuster to improve flotation bubbles.

2. Experimental

2.1. Materials

The quartz samples used in the tests were purchased from Heyuan City, Guangdong Province, China. After crushing, sieving, and selecting, they were ball-milled to a size below 106 μm using a planetary ball mill under corundum medium. The samples were washed with hydrochloric acid to remove all contamination, then washed with ultrapure water and dried for later use. The hematite was from South Africa, with all magnetic parts removed by magnetic separation. The samples were also prepared to below 106 μm. The raw ore used in the artificial mixed ore flotation tests was made from hematite and quartz in a mass ratio of 2:1. This ratio was chosen to approximate the grade of banded hematite in nature. In all flotation experiments, only particles with a size range of 37–106 μm were used for flotation, and those below 37 μm were screened out. This study aimed to exclude the influence of fine mud on the adsorption and bubble generation to facilitate the analysis of the underlying mechanisms. The compositions of quartz and hematite are listed in Table 1.
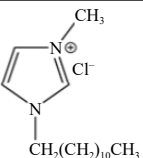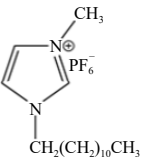
The Lanzhou Institute of Physics, Chinese Academy of Sciences, provided two types of ILs used in the experiments and other reagents needed in the experiment were purchased from the Sinopharm Group. All reagents were analytically or spectrally pure. The two ILs used in the experiments were

Table 1. Chemical compositions of the minerals wt%

Minerals	TFe	SiO_2	Na_2O	Al_2O_3	CaO	MgO	P_2O_5
Quartz	0.05	99.840	0.009	0.050	0.0012	0.013	0.004
Hematite	69.29	0.402	0.059	0.239	0.0400	0.047	0.067

Table 2. ILs used and the phychemical property

Name	Structure	Molecular mass / (g·mol^{-1})	MP / °C	lg$P$	PSA / nm^2
1-dodecyl-3-methylimidazolium chloride (C$_{12}$[mim]Cl)		286.88	96	1.24	8.81
1-dodecyl-3-methylimidazolium hexafluorophosphate(C$_{12}$[mim]PF$_6$)		396.40	50	7.62	22.40

Note: *P* represents the oil–water coefficient.

C$_{12}$[mim]Cl and C$_{12}$[mim]PF$_6$, and their brief information is presented in Table 2. MP indicates the melting point of the substance, lg$P$ represents the oil–water partition coefficient, and PSA denotes the polar surface area. Both are collectors and frothers in the flotation experiments. These two reagents were diluted with ultrapure water and EtOH to a specified concentration and added to the pulp in proportion to the flotation. C$_{12}$[mim]PF$_6$ has strong hydrophobicity, and its aqueous solution must be heated during preparation and used after cooling. No heating is required when using EtOH to prepare the C$_{12}$[mim]PF$_6$ solution.

2.2. Flotation

The flotation cell, named XFG-5, used in all the flotation experiments was a hanging-trough flotation machine produced by Wuhan Prospecting Machinery Factory with a rated capacity of 60 mL. Various conditions for the flotation test were determined through preliminary exploratory tests. The pulp concentration was 10wt%. The float was rotated at 1300 r/min, and the stirring time was 3 min. Stirring was continued for 3 min after adding the ILs, followed by scraping the bubbles for 3 min after turning on the aeration device. The resulting tailings and concentrates were filtered and dried using a suction filter and oven, and the iron composition was analyzed by standard titration. All flotation experiments were performed using ultrapure water.

2.3. Foaming study

Foam stability tests were performed in a foam-generating column, and the experimental apparatus was independently assembled using the gas flow method, which was assembled following literature [31]. The main components were an inflation apparatus, a gas velocity measurement apparatus, a foam column, and a silicone tube. In the experiment, a peristaltic pump was chosen as the inflationary device, considering the inflation rate and stability. The gas velocity measurement device used was a rotor flow meter. The foam column is customized on the basis of a chromatographic column and has a scale. To prevent leakage of the testing solution while sufficiently separating the gas, a quartz sand core with a pore size of 15–30 μm (G3 sand core) was selected at the bottom of the foam column. A camera recorded changes in the foam height.

During the tests, the gas flow velocity was maintained at 600 mL/min, and 50 mL preprepared ILs was poured into the foam column as a frother. When the liquid was stabilized, the air pump was turned on for aeration and stopped after 60 s. The foam height and defoaming time were then observed. After completing the experiment, the device was cleaned, and the next set of tests was performed.

2.4. Instrument characterization

The quartz samples used in the Fourier transform infrared (FT-IR), and X-ray photoelectron spectroscopy (XPS) tests were prepared by stirring the IL solution with quartz. The stirring equipment used was a magnetic stirrer, and the IL concentration was 4×10^{-5} mol·L^{-1}. A sample with EtOH as the solvent was equivalent to adding the corresponding concentration of EtOH. The rotational speed of the magnetic stirrer was set to 500 r/min, and the stirring time was 30 min. After stirring, the samples were suction filtered, washed, and thoroughly dried at room temperature in a vacuum drying oven.

The device used in the XPS study was the ESCALAB 250Xi/ESCALAB 250Xi manufactured by Thermo Fisher Scientific. Polyvinyl alcohol (PVA) was used as the sample preparation binder. The test pressure was kept below 5×10^{-6} Pa with a single 500 μm X-ray spot. The anode was selected as aluminum, and the monitoring values were approximately 14.2 kV and 11.3 mA, respectively. The instrument used for the FTIR analysis was a Nicolet 6700 FT-IR with a test wavenumber range of 400–4000 cm^{-1}. The sample was mixed with KBr at a weight ratio of 1:100, ground to less than 5 μm, and post-stamped. Malvern Zeta Sizer Zeta-Nano (ZS90, Malvern, UK) was used to test the Zeta potential of quartz after IL adsorption. Mineral samples were ground to less than 5 μm, and 100 mg of the sample was added to 100 mL of 5% EtOH solution. The concentration of the IL collector to the target concentration was adjusted and then tested after ultrasonic dispersion. The Zeta potential test was completed using the Scientific Compass.

3. Results and discussion

3.1. Flotation test results

Two ILs were dissolved using ultrapure water and EtOH

as solvents and utilized as collectors for the flotation tests of pure quartz and hematite. Fig. 1 presents the flotation results of pure quartz and high-purity hematite. The error bar represents the standard deviation between the results of more than three experiments, and the t-test presented in Table 3 shows the differences in the quartz recovery between EtOH and H_2O. The flotation results of high-purity hematite were obviously different; therefore, the data were not analyzed for differences.

In Fig. 1(a)–(b), EtOH improved the quartz recovery of the $C_{12}[mim]Cl$ collector with the IL concentrations of 0.01 and 0.02 mM. When the concentration was increased, quartz recovery remained above 90%, but it was lower than that obtained under water solvent conditions. The $C_{12}[mim]PF_6$ collector differed from $C_{12}[mim]Cl$. When the $C_{12}[mim]PF_6$ concentrations were 0.01 and 0.02 mM, quartz recovery in the EtOH solvent decreased. When the collector concentration increased, quartz recovery increased closely to that of the water solvent. In the higher IL concentration range, the quartz recovery rate of $C_{12}[mim]Cl$ (EtOH) was always lower than that of $C_{12}[mim]Cl$ (H_2O), and the quartz recovery of $C_{12}[mim]PF_6$(EtOH) did not decrease as in water due to multilayer adsorption when the reagent concentration was too high. In Fig. 1(c)–(d), the disparities between the two types of ILs were more pronounced. Throughout the entire concentration range, EtOH resulted in greater flotation of hematite when using $C_{12}[mim]Cl$ as a collector. Conversely, the presence of EtOH decreased the flotation recovery of hematite when $C_{12}[mim]PF_6$ was used.

In flotation tests of low concentration of $C_{12}[mim]PF_6$ (EtOH), whether quartz or hematite was present in the pulp, the froth was more numerous, brittler, and smaller compared with $C_{12}[mim]PF_6$ (H_2O). Stable mineralized bubbles were almost unobservable, which should be the direct reason for the decrease in quartz recovery. Simultaneously, the flotation recovery of hematite with $C_{12}[mim]PF_6$ (EtOH) decreased greatly across all concentrations. However, the natural floatability of quartz surpasses that of hematite. Therefore, as the concentration of $C_{12}[mim]PF_6$ (EtOH) increases, the recovery of quartz approaches that of $C_{12}[mim]PF_6$ (H_2O). The difference was that well-mineralized foam had already been observed with $C_{12}[mim]Cl$ (EtOH) in the low-concentration range. Although the bubble life was shorter, it was due to the low IL concentration. The stability of these foams was still higher than that of $C_{12}[mim]PF_6$ (H_2O) and sufficient to float quartz and hematite.

Reverse flotation tests of mixed ore were also carried out using 2:1 mass ratio of hematite and quartz as raw ore. No inhibitors were used in the experiments. The flotation test results are shown in Fig. 2.

EtOH resulted in a decrease in the concentrate grade and recovery of the $C_{12}[mim]Cl$ collector compared with the $C_{12}[mim]Cl$ (H_2O) collector in the mixed ore flotation. At a $C_{12}[mim]Cl$ concentration of 0.16 mM (EtOH concentration
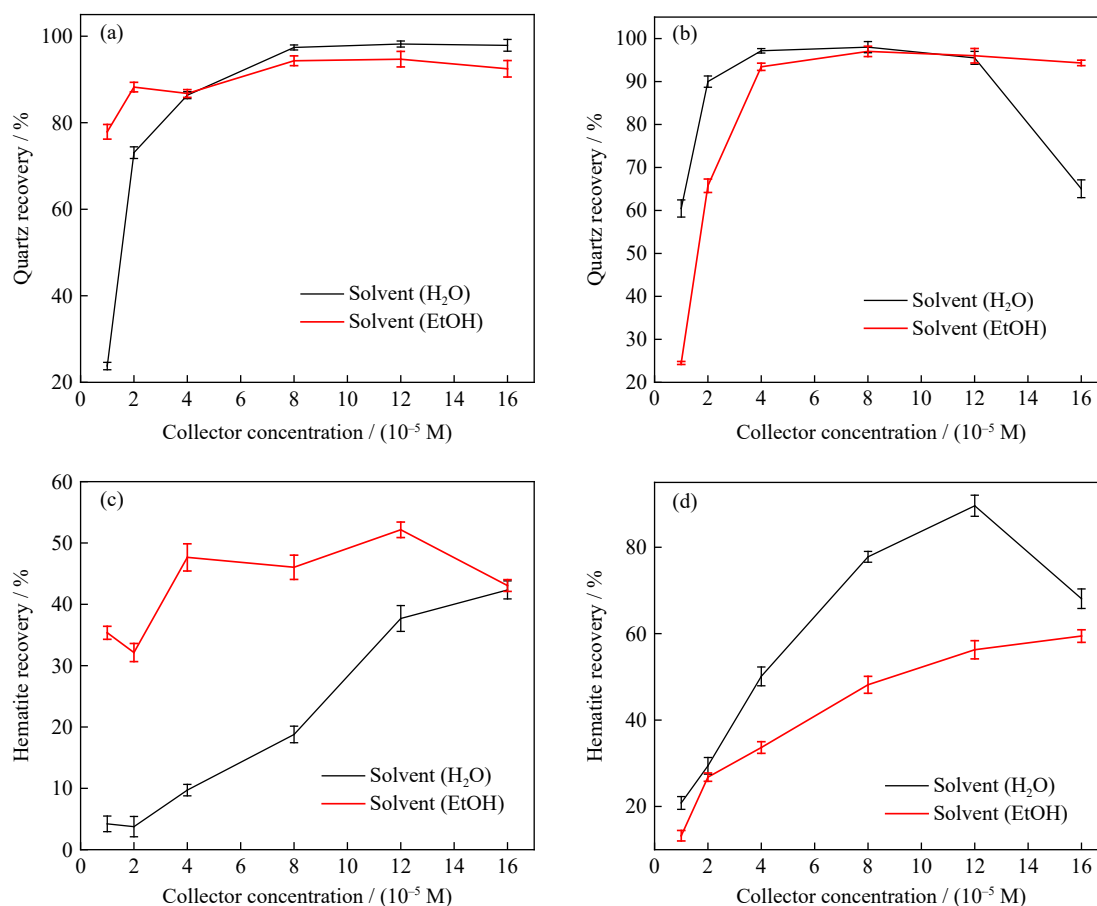

Fig. 1.   Variation of quartz and hematite flotation recovery with different IL concentration: (a, c) $C_{12}[mim]Cl$; (b, d) $C_{12}[mim]PF_6$.

Table 3. Results of the t-test of statistics about quartz recovery in Fig. 1(a)–(b)

Collector concentration / (10^{-5} M)	Results of the t-test of statistics	
	C_{12}[mim]Cl	C_{12}[mim]PF$_6$
1	0	0
2	0.0001	0
4	**0.6067**	0.0028
8	0.0140	**0.3917**
12	0.0347	**0.7262**
16	0.0159	0

of 16%), the concentrate recovery decreased to 20%. During the experiments, the addition of EtOH had a positive effect on the bubbles of C_{12}[mim]Cl. Considering the results of flotation tests of quartz and hematite, the preliminary speculation was that more bubbles caused additional hematite to be entrained, resulting in a decrease in selectivity, concentrate grade, and recovery.

However, the performance of C_{12}[mim]PF$_6$ (EtOH) differed from C_{12}[mim]Cl. Previous studieshave discussed that C_{12}[mim]PF$_6$ (H$_2$O) exhibits excessively strong collecting capacity, causing both quartz and hematite to float, which then leads to low flotation efficiency [29]. However, in the experiments with the C_{12}[mim]PF$_6$ (EtOH) collector, the grade and recovery of the concentrate increased at the same time. The froth during the C_{12}[mim]PF$_6$ (EtOH) flotation was fine and fragile, consistently forming and breaking rapidly. The scraping of foam also led to quick defoaming. Considering the results of the flotation tests of quartz and hematite, EtOH was speculated to cause the flotation bubbles of C_{12}[mim]PF$_6$ to become fragile under the action of a certain mechanism. The secondary enrichment effect was strengthened, and the flotation efficiency of the C_{12}[mim]PF$_6$ (EtOH) collector was improved in the absence of an inhibitor.

As EtOH participated in flotation in the form of IL solvents, the amount of EtOH actually increased when the number of ILs was increased. Therefore, the above experiments have two variables: IL collector concentration and

EtOH concentration. EtOH affects the flotation, but the experimental results cannot be analyzed from the perspective of single-factor experiments. Two additional pure quartz flotation tests were thus conducted. In the first experiment, the IL collector concentration was fixed at 0.01 mM, and the EtOH concentration was used as a variable. For another set of experiments, the EtOH concentration was fixed at 2%, and the IL concentration was variable. These two concentrations were chosen to create a substantial contrast in the flotation results of these two IL collectors, facilitating convenient analysis. The results are illustrated in Fig. 3.

The flotation results in Fig. 3(a) imply that the quartz recovery of the C_{12}[mim]Cl collector showed stability at EtOH concentrations of 1%–3% but decreased slowly after EtOH increased more than 3%. For C_{12}[mim]PF$_6$ of low concentration, the addition of EtOH significantly weakened the collecting capacity. As the EtOH concentration increased, the quartz recovery improved slightly, but the maximum recovery was only approximately 40%. When the EtOH concentration exceeded 4%, the quartz recovery of C_{12}[mim]PF$_6$ also entered a declining stage similar to that of C_{12}[mim]Cl.

In Fig. 3(b), the quartz recovery of low-concentration C_{12}[mim]PF$_6$ was lower than that of C_{12}[mim]Cl. As the concentration of C_{12}[mim]PF$_6$ increased, the quartz recovery gradually improved, and finally close to C_{12}[mim]Cl reached more than 90%. Through the analysis of these two groups of tests combined with pure quartz flotation tests, EtOH apparently has a negative impact on the flotation efficiency of the C_{12}[mim]PF$_6$ collector. Even C_{12}[mim]PF$_6$ of high concentrations could not exceed the quartz recovery of C_{12}[mim]Cl when EtOH was maintained at 2%.

3.2. Froth observation and analysis

After EtOH affected the C_{12}[mim]Cl and C_{12}[mim]PF$_6$ collectors, the changes in the flotation results showed contradictions. The most significant difference between these two ILs was observed in their flotation froth when EtOH was used. Both showed enhanced froth volume during the flotation when EtOH was present. The difference was that the froth of C_{12}[mim]Cl maintained viscosity and could
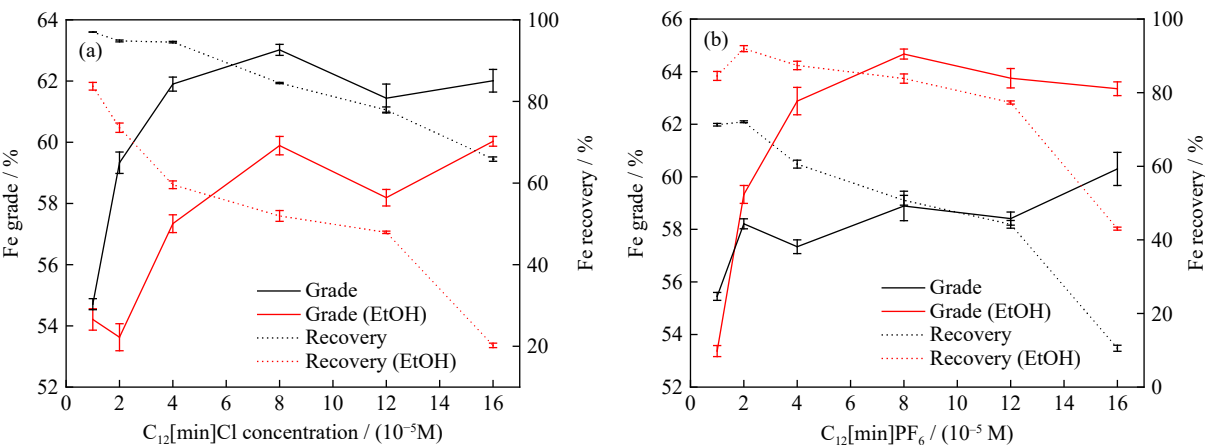

Fig. 2. Variation of hematite and quartz mixed ore flotation separation results with IL concentration: (a) C_{12}[mim]Cl; (b) C_{12}[mim]PF$_6$.
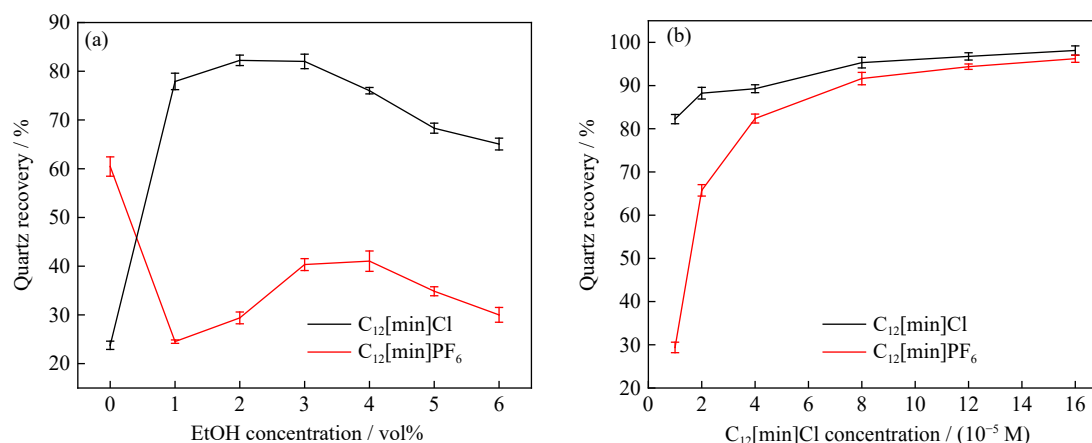
Fig. 3.   Pure quartz flotation test recovery as a function of (a) EtOH concentration and (b) ILs concentration.

float ore, whereas the froth of $C_{12}[mim]PF_6$ at low concentration became brittle, constantly generated and broke, and could not be scraped stably. Its froth became stable only when the concentration of $C_{12}[mim]PF_6$ increased, which can be attributed to the fact that $C_{12}[mim]PF_6$ stabilized the foam. The phenomenon of brittle froth like this is obviously related to EtOH. Considering that the froth of $C_{12}[mim]Cl$ under the same concentration did not exhibit this behavior, speculating that PF_6^- played a key role was easy. To analyze more changes in the froth, experiments were conducted for two-phase foam observation. The results are shown in Fig. 4.
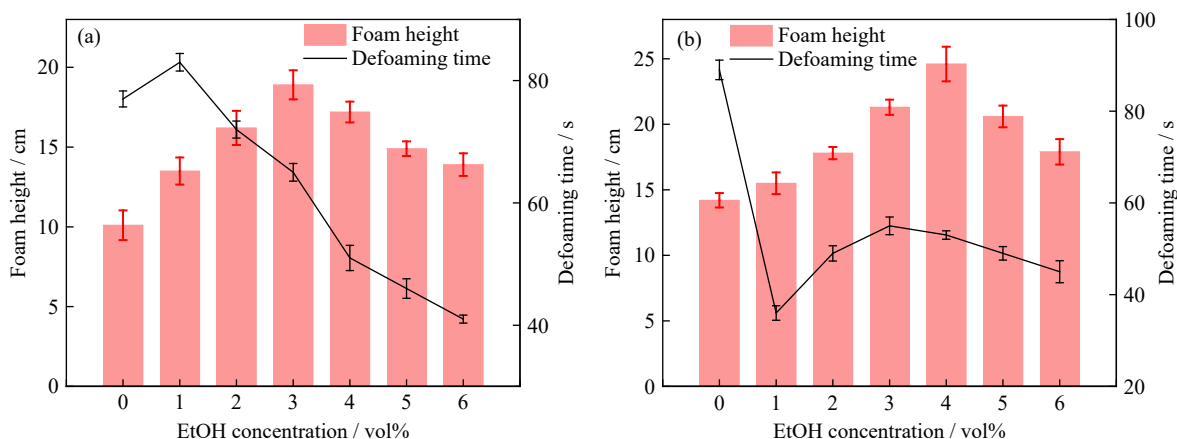

Fig. 4.   Two-phase foam as a function of EtOH concentration with ILs at a concentration of 10×10^{-5} mol·L^{-1}: (a) $C_{12}[mim]Cl$; (b) $C_{12}[mim]PF_6$.

ILs were used as frothers at a concentration of 10×10^{-5} M to obtain more froth for observation. The bar graph in Fig. 4 shows the froth height after 60 s of aeration, corresponding to the left axis. The line chart shows the defoaming time after the air pump was turned off, corresponding to the right axis.

$C_{12}[mim]PF_6$ has better foaming power than $C_{12}[mim]Cl$ in water solvent. When EtOH was added, the froth height of $C_{12}[mim]Cl$ increased but gradually decreased as the EtOH concentration exceeded 3%. At the same time, the static defoaming time gradually decreased after the air pump was turned off, which meant that the stability of the static foam decreased. For $C_{12}[mim]PF_6$, the foam height exhibited minor changes at low EtOH concentrations. With the continuous increase in EtOH concentration, the dynamic foam height initially increased and then decreased. In addition, after aeration was stopped, the defoaming time for the static foam was significantly shortened compared with that for no EtOH. With the increase in EtOH concentration, the defoaming time showed a slight increase before entering a decreasing trend

again.

In summary, the dynamic foam represented by the foam height showed little difference between the two ILs. EtOH promoted foam froth before the concentration exceeded 3%–4%. A higher concentration of EtOH caused the foam height to decrease, but it remained higher than the dynamic foam height without EtOH. However, the defoaming time showed that the static foam stability was different between the two ILs. The defoaming time for static foam after aeration was stopped was negatively affected by EtOH for both ILs, but the static foam of $C_{12}[mim]PF_6$ was more affected than $C_{12}[mim]Cl$, consistent with the phenomenon observed in the flotation experiments.

Studies have analyzed the bubble behavior of water solutions of EtOH in a bubble column [32–33]. Andrew was the first to propose a dynamic surface tension model to explain how EtOH affects bubbles in water [34]. The stability of bubbles ultimately depends on the rheological properties of the liquid film and the interbubble mechanics, whether they

are affected by EtOH or by IL surfactants [35]. The surface chemistry fundamental revealed that EtOH would accumulate at the gas–liquid interface when it is added to a solution [36]. The dynamic surface tension model indicated that EtOH adsorption on the bubble surface differed from that of the conventional frother and was not firmly adsorbed. As the solution was agitated, the bubbles moved, deformed, and expanded within the liquid, which caused the density of adsorbed EtOH on the bubble surface to decrease and the surface tension of the gas–liquid interface to increase dynamically. Consequently, a surface tension gradient was created at the gas–liquid interface, which caused the liquid to move under the influence of this gradient, increasing the thickness of the liquid film and stabilizing it. This process is illustrated in the left half of Fig. 5.

Compared with the "EtOH + H_2O" system studied in the above studies, in the flotation pulp, IL surfactants could stabilize bubbles, and minerals could be adsorbed on the bubble surface, enhancing the strength of the three-phase foam [37]. Assisted by the dynamic surface tension effect induced by EtOH, even at a concentration as low as 1×10^{-5} M, $C_{12}[mim]Cl$ could strongly inhibit bubble coalescence during the perturbed ascent, leading to significant froth formation and maintaining foam viscosity during flotation. However, the foam enhanced by EtOH does not exhibit adsorptive selectivity like the foam stabilized by ILs. This indiscriminate foam enhancement caused significant entrainment in the reverse flotation tests of mixed ores, resulting in the flotation of a large amount of hematite [38]. This deteriorated the flotation separation effect of the mixed ores with the $C_{12}[mim]Cl$ collector.

The situation of $C_{12}[mim]PF_6$ differed from that of $C_{12}[mim]Cl$. As analyzed in the first paragraph of this section, that PF_6^- played a crucial role in this different flotation performance could be easily speculated. PF_6^- is a strongly hydrophobic anion, and studies have shown that the hydrogen bond binding energy between PF_6^- and water is positive [39–40]. PF_6^- in an aqueous solution can only exist in the cavities of water molecules. When preparing $C_{12}[mim]PF_6$ solution with water as a solvent, stable solution could only be achieved by heating and stirring and only exists at low concentrations [29]. This low solubility still exists because of the slight hydrophilicity of the cationic head group. However, when preparing a $C_{12}[mim]PF_6$ solution using EtOH as the solvent and adding it to the flotation pulp, EtOH aggregate near PF_6^-, connecting one end to PF_6^- and the other end to water molecules, thereby integrating PF_6^- into the hydrogen bond network of water molecules [41]. Combined with the flotation tests phenomenon, when PF_6^- was adsorbed near the bubble surface by the electrostatic force with the imidazole IL cation, EtOH around PF_6^- would integrate into the bubble surface, causing local abnormal aggregation of EtOH at the bubble surface, leading to a decrease in surface tension in this area and producing a surface tension gradient. The direction of the force generated by this surface tension gradient is exactly opposite to the tension gradient caused by EtOH when it enhanced the froth. Therefore, the surface tension of the bubble was unbalanced, the liquid film became thinner, and the froth broke. This process is shown on the right side of Fig. 5.
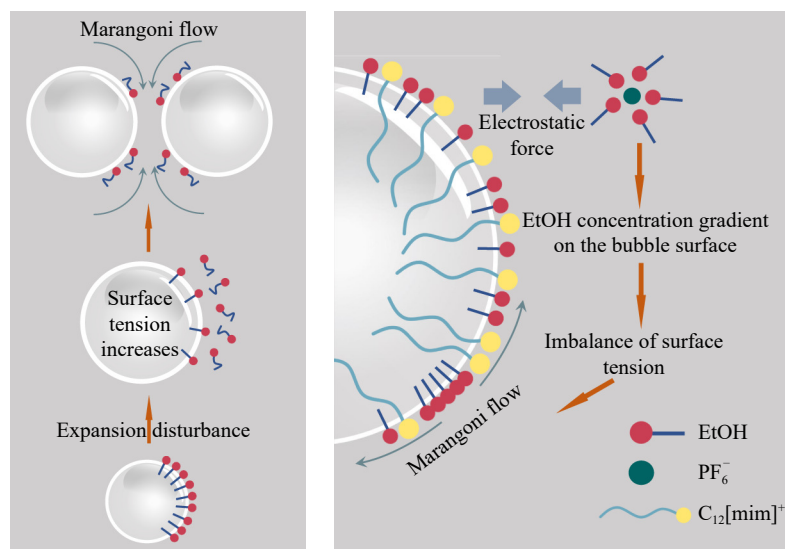

Fig. 5.   Diagram of ethanol affecting flotation bubbles.

According to the flotation fundamental [37], various factors such as dehydration of the froth layer, bubble coalescence, reduction of the gas–liquid interface, and turbulence caused by bubble wall rupture can cause mineral particles adhered to the gas–liquid interface to compete for attachment on the bubble surface based on their adhesion strength. This phenomenon is the secondary enrichment effect.

In the mixed ore flotation, the surface tension gradient effect of EtOH enhanced the stability of the froth, whereas the aggregation of EtOH on the bubble surface driven by PF_6^- reduced the stability of the froths, causing them to become brittle and rupture. These two processes accelerated the cyclic process of the "generation and breaking" dynamic equilibrium of flotation frothing. This phenomenon was signific-

antly beneficial for the occurrence of the secondary enrichment effect. As two kinds of minerals with similar hydrophilicity and negative surface potential, hematite has a higher surface potential than quartz, making it less floatable than quartz when using cationic collectors [42]. Therefore, after the secondary enrichment effect was strengthened by EtOH, C_{12}[mim]PF_6 was used as a collector in the mixed ore flotation test without using any inhibitor to achieve good mixed ore separation results.

In addition, as the concentration of EtOH in the flotation pulp increased, the EtOH distribution in the pulp tended to be homogeneous. The EtOH concentration on the bubble surface stabilized. Although the dynamic surface tension effect was weakened and the promoting effect of EtOH on bubble stabilization was reduced, the bubble annexation was still less than that without EtOH. When the EtOH concentration exceeded 3% and 4%, the froth height decreased, which indicated an increase in bubble mergers. This concentration is consistent with some research results on the behavior of bubbles in the bubble column of ethanol-water solutions [32]. The froth height reached a maximum of 4% for C_{12}[mim]PF_6 and 3% for C_{12}[mim]Cl. This difference may be due to EtOH aggregated around PF_6^-, resulting in a decrease in the amount of EtOH involved in the formation of the surface tension gradient, and more EtOH was needed to maximize the froth height of C_{12}[mim]PF_6. Nonetheless, more evidence is needed to make a definite conclusion regarding this detail.

This dynamic surface tension effect depended on the disturbance of the pulp and had little effect on the static foam after aeration was stopped. However, the anomalous accumulation of EtOH on the bubble surface caused by PF_6^- and the resulting bubble rupture process were not influenced by the pulp being stationary or disturbed. As shown in Fig. 4, the defoaming time of static bubbles of C_{12}[mim]PF_6 rapidly decreased at an EtOH concentration of 1%. This corresponded to the weak collecting capacity of C_{12}[mim]PF_6 in Fig. 3(a) at the same concentration and the consistently lower quartz recovery of C_{12}[mim]PF_6 than C_{12}[mim]Cl at an EtOH concentration of 2% in Fig. 3(b). As the EtOH concentration increased to 3%–4%, EtOH gradually became homogeneous in the pulp, and the effect of bubbles became brittle caused by PF_6^- weakened. In Fig. 4, the defoaming time slightly increased for the static foam, corresponding to a partial improvement in the quartz recovery of C_{12}[mim]PF_6 in Fig. 3(a) at EtOH concentration of 3%.

As the EtOH concentration increased to 5%–6%, the defoaming time for C_{12}[mim]PF_6 decreased again. At the same time, for C_{12}[mim]Cl, as the EtOH concentration increased from 2%, the defoaming time shortened, and the stability of its static bubbles worsened. The quartz recovery of C_{12}[mim]Cl (EtOH) in the high concentration range of the pure quartz tests in Fig. 1 was lower than that of C_{12}[mim]Cl (H_2O). This phenomenon was speculated to be due to the excessive solvation of the IL cations in the solution caused by EtOH. Further discussion on this topic will be conducted in the following section.

3.3. Solvation

During flotation, the ILs served both as collectors and frothers. The frothing process of ILs as a frother and the modification of ore surface properties as collectors depend on the adsorption of cationic moieties on the froth or ore surface [43]. Electrostatic repulsion between the cationic head groups decreases the adsorption density and efficiency. Stable bubbles or complete alteration of the surface properties of minerals can only be achieved through the formation of semimicelle adsorption, where the cationic groups are adsorbed in clusters on the surface of minerals or bubbles [29]. The formation of semimicelle adsorption depends on the balance between two effects: electrostatic repulsion between the cationic head groups and hydrophobic interaction between the alkyl chains that induce attraction. Electrostatic repulsion weakens aggregation, whereas hydrophobic interaction strengthens the tendency to aggregate.

The Cl$^-$ or PF_6^- anions can approach the cation under the action of electrostatic force to form ion pairs, which weaken the electrostatic repulsion, promote the formation of semimicelles, and enhance the adsorption of ILs on mineral or foam surfaces. Our previous research has analyzed this phenomenon [29]. The addition of EtOH affected the hydrophobic interaction between alkyl chains. EtOH can act as a bridge between alkyl chains and solvent water to enhance the solvation of alkyl chains, promote the alkyl chain of the IL cation to join the hydrogen bond network of water, and reduce the system's energy. The hydrophobic interaction between alkyl chains is then reduced, resulting in a decrease in the self-assembly ability of the IL and a decrease in the adsorption density of IL cations on mineral or bubble surfaces.

Studies have analyzed the influence of EtOH on the self-assembly ability of ILs in water [44–46]. The addition of EtOH increases the critical micelle concentration of ILs in water through "promoting solvation" and reduces the number of aggregates. As a "colloid aggregation phenomenon" that occurs in the ore or bubble surface, semimicelle adsorption is also affected by this process, but it occurs at a much lower concentration than critical micellization concentration (CMC).

In the foam analysis section, the aggregation of EtOH around PF_6^- was due to the hydrogen bond energy between PF_6^- and water being positive [39], which represents the absolute hydrophobicity of PF_6^-. PF_6^- is often encapsulated in "holes" formed by ordered water molecules in pure water and easily bound to the carbon chain cation through an entropy-driven process. This is also why it has good collecting capacity and foam ability in water solvents [29]. The addition of EtOH also has a solvation effect on PF_6^-, so C_{12}[mim]PF_6 is influenced by the "dual" solvation effect of EtOH on the anion and cation. However, the anion Cl$^-$ of C_{12}[mim]Cl has better water solubility, so it can be roughly assumed that only the cation is affected by the EtOH solvation. This process is briefly described in Fig. 6.

Based on the above analysis, with the increase in EtOH concentration in the pulp, the "solvation effect" gradually
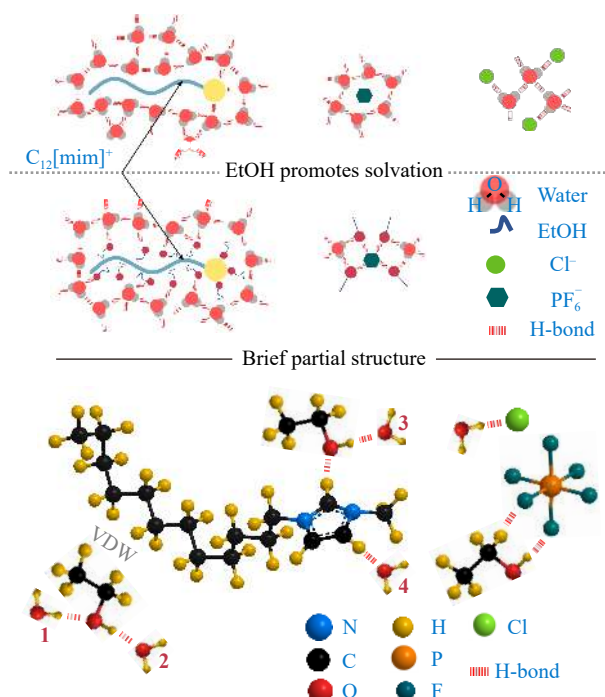
Fig. 6.   Rough sketch of the ethanol-promoted solvation of ILs in water.

strengthens, leading to a decrease in the adsorption of the cations of both ILs on the bubble surface and an acceleration in the froth merging. However, in the case of C_{12}[mim]PF_6 froth, this process interfered with low EtOH concentrations due to the influence of PF_6^-. When the collector concentration was increased synchronously with the EtOH concentration in Fig. 1, the increase in collecting capacity due to concentration weakened the solvent effect caused by EtOH. Nevertheless, the t-test in Table 3 confirmed that the quartz recovery of C_{12}[mim]Cl (EtOH) remained lower than that of C_{12}[mim]Cl (H_2O) in the high concentration range. In Fig. 3(a), as the concentration of EtOH continuously increased while the IL concentration remained unchanged, the quartz recovery would continuously decrease. This was caused by "foam viscosity decay" and "collection ability decay," both attributed to the influence of EtOH.

This weakening of the collecting capacity does not always have a negative impact. For example, in the previous research [29], the selectivity of C_{12}[mim]PF_6 is poor due to its excessive collecting power. After adding EtOH, its collecting capacity is appropriately reduced, and a better concentrate grade and concentrate recovery rate can be achieved without a collector through the influence on the froth.

Compared with "foam viscosity decay," "collector capability decay" is more easily validated through adsorption-related characterization tests. Therefore, FTIR, XPS, and Zeta potential analyses were performed on quartz treated with ILs (EtOH) to confirm that EtOH reduced the adsorption of ILs on the surface of quartz.

3.3.1. FT-IR results

The IR spectra of pure quartz and quartz treated with both ILs are shown in Fig. 7. In contrast to pure quartz, the new peaks around 2900 cm^{-1} were characteristic peaks of –CH$_2$–

and –CH$_3$, which were the absorption peaks of the carbon chain of ILs, indicating the adsorption of imidazolium ILs on the ore surface. According to the observations of the enlarged part, after the ILs were adsorbed on the quartz surface, the carbon chains of the alkyl chains of the collector molecules were affected by the van der Waals force and approached each other, resulting in intermolecular forces. As a result, the stretching vibration of the –CH$_2$– peak weakened, and the wave number decreased. Thus, more adsorption led to denser alkyl chains, so the van der Waals forces between the carbon chains became stronger, and the stretching vibrations of the methylene peaks weakened. The change in the wavenumber of the methylene absorption peak indicates the degree of quartz adsorption. The surface methylene groups of quartz treated with C_{12}[mim]Cl and C_{12}[mim]PF_6 in EtOH solvent shifted to the higher wavenumber direction. This phenomenon indicates that the adsorption of both ILs on the quartz surface decreases in the presence of EtOH.
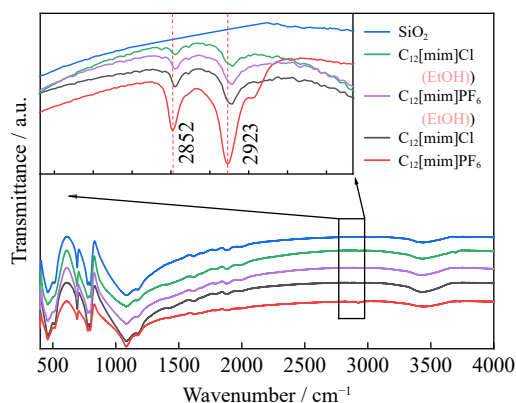

Fig. 7.   FT-IR spectra of the IL-treated quartz.

3.3.2. XPS analysis

The quartz ore samples prepared and processed in the same way as FT-IR were analyzed through XPS, and the corresponding spectrum was obtained. The peak spectrum of N 1s is listed in Fig. 8.

The N peak in the XPS spectrum at the quartz surface rose entirely from the adsorption of nitrogen-containing ILs. The more IL molecules were adsorbed, the larger the relative peak area of N 1s. Observing the peak spectrum of N 1s in Fig. 8, compared with the N 1s peak under the aqueous solution condition, the two ILs under the ethanol solvent condition exhibited a hardly noticeable N 1s peak. This illustrates the decrease in IL adsorption on the quartz surface under ethanol conditions.

Table 4 lists the peak area ratios of N and Si in the XPS peak spectra, and the N/Si atomic concentration ratio can be viewed as an intuitive expression of the degree of IL adsorption on the quartz surface. Both collectors had higher N/Si ratios in the water solvent condition, indicating that more ILs (H_2O) were adsorbed on the ore surface. The peak positions of N 1s showed that the N 1s binding energies of the two ILs (EtOH) were lower than those in the water solvent. After the addition of EtOH, the solvation effect takes place, the ad-
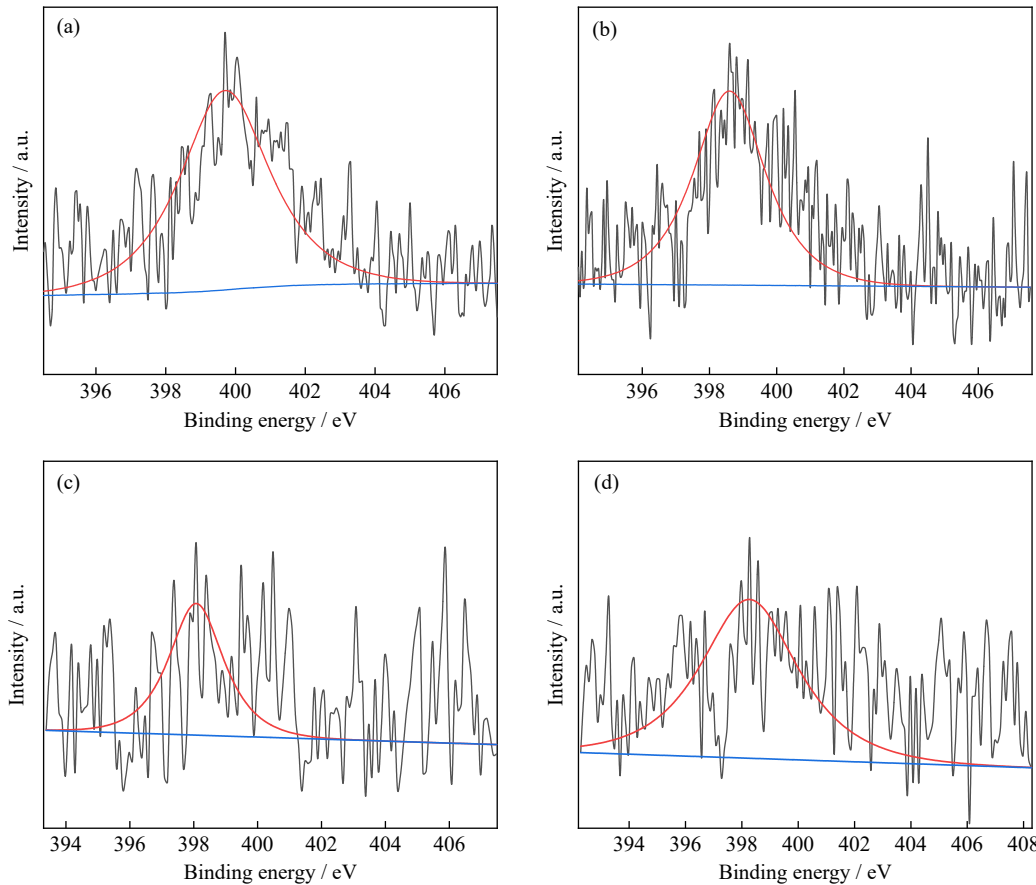
Fig. 8.   XPS spectra of N 1s of quartz treated with different ILs: (a) C_{12}[mim]Cl; (b) C_{12}[mim]PF_6; (c) C_{12}[mim]PF_6 (EtOH); (d) C_{12}[mim]Cl (EtOH).

Table 4.   N/Si peak area ratios in the XPS analysis

Solvent	IL Collectors	N/Si peak area ratio (N × 100/Si)	N
H₂O	C_{12}[mim]Cl	7.12	399.7
	C_{12}[mim]PF_6	13.09	398.6
EtOH	C_{12}[mim]Cl	1.92	398.08
	C_{12}[mim]PF_6	4.22	398.28

Fig. 9.   Zeta potential of the quartz surface treated with different collectors.

sorbed ILs on the quartz surface are "screened," and the weakly adsorbed ILs are detached. Only ILs under the action of super-strong electrostatic force are partially adsorbed to the quartz surface, so ILs adsorbed on the quartz surface have the characteristics of high electron density in the outer layer, and the shielding effect is strengthened. Under the push electron effect, the electron combination of N 1s can be lower.

3.3.3. Zeta potential results

During the Zeta potential test, the EtOH concentration was maintained at 5%, and the IL concentration was adjusted for testing. The results are shown in Fig. 9. In the range of low collector concentrations, the surface Zeta potential of IL (EtOH)-treated quartz was already lower. With an increase in the concentration of ILs, the Zeta potential of the quartz surface changed rapidly. EtOH significantly slowed down the speed of this potential change, requiring a higher concentration of ILs to shift the quartz surface potential from negative to positive. As the concentration of ILs continued to increase, the effect of EtOH weakened. The concentration of
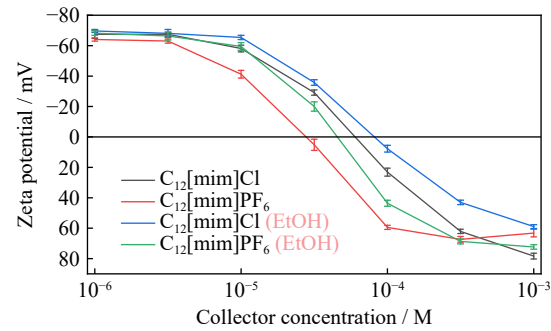
C_{12}[mim]PF_6 (EtOH) required to change the Zeta potential of the quartz surface from negative to positive was lower than that of C_{12}[mim]Cl (EtOH), which indicates that the collection property of C_{12}[mim]PF_6 (EtOH) was still stronger than that of C_{12}[mim]Cl (EtOH). However, the low concentration of C_{12}[mim]PF_6 (EtOH) was poor in the pure mineral flotation test, which further explained that the relatively stable bubbles of C_{12}[mim]Cl had a greater impact on the flotation test results.

4. Conclusions

This study found that the flotation results of two ILs with similar structures are quite different under the influence of EtOH and attempted to explain the reason through foam and

solvation analyses. The beneficial and unfavorable effects of the addition of EtOH on the flotation with ILs as collectors are discussed, providing possibilities for the reagent regime of imidazolium ILs used as collectors for flotation.

In general, an appropriate concentration of EtOH can reduce bubble merger and enhance foam stability in the flotation for hydrophilic IL collectors. This effect is most pronounced when the EtOH concentration is 3%–4%. This is caused by the dynamic surface tension gradient effect resulting from the dynamic desorption of EtOH from the bubble surface during pulp disturbance.

For hydrophobic ILs, EtOH can expedite the "generation and breaking" cyclic process of flotation frothing, promote the occurrence of secondary enrichment, and improve its selectivity without any inhibitor. The abnormal accumulation of PF_6^- driven EtOH on the flotation froth surface is the reason for this phenomenon.

Moreover, EtOH can reduce the froth viscosity after it is scraped out, thereby reducing the defoaming time. The solvation effect of EtOH on the ILs causes such a reduction. In association with the reduced bubble merger effect during aeration, the benefit of enhancing the frothing in pulp and quickly defoaming the scraped foam can be achieved.

The disadvantage caused by this solvation is that the adsorption capacity of ILs on the ore surface and bubble surface weakens, resulting in less adsorption of ILs (EtOH) on the ore surface, as observed in FT-IR, XPS, and Zeta potential analyses. However, this solvation and the benefit of EtOH in the flotation froth did not occur within the same concentration range. In actual production, using even 16% EtOH in the pulp, as in the flotation tests, is impractical. Therefore, an appropriate concentration of EtOH can effectively regulate the flotation of hydrophilic and hydrophobic IL collectors.

Acknowledgements

Conflict of Interest

The authors declare that they have no known competing financial interests or personal relationships that could have appeared to influence the work reported in this paper.

References

[1]   K.R. Seddon, A taste of the future, *Nat. Mater.*, 2(2003), No. 6, p. 363.

[2]   S.A. Forsyth, J.M. Pringle, and D.R. MacFarlane, Ionic liquids—An overview, *Aust. J. Chem.*, 57(2004), No. 2, art. No. 113.

[3]   Y.L. Wang, H.Y. He, C.L. Wang, *et al.*, Insights into ionic liquids: From Z-bonds to quasi-liquids, *JACS Au*, 2(2022), No. 3, p. 543.

[4]   B.A.D. Neto and J. Spencer, The impressive chemistry, applications and features of ionic liquids: Properties, catalysis & catalysts and trends, *J. Braz. Chem. Soc.*, 23(2012), No. 6, p. 987.

[5]   Y. Liang, S.X. Bao, Y.M. Zhang, B. Chen, and C. Yu, Adsorption behavior of vanadium using supported 1-butyl-3-methylimidazolium chloride ionic liquid, *Miner. Process. Extr. Metall. Rev.*, 45(2024), No. 3, p. 238.

[6]   B.Y. Liu and N.X. Jin, The applications of ionic liquid as functional material: A review, *Curr. Org. Chem.*, 20(2016), No. 20, p. 2109.

[7]   W.J. Qian, J. Texter, and F. Yan, Frontiers in poly(ionic liquid)s: Syntheses and applications, *Chem. Soc. Rev.*, 46(2017), No. 4, p. 1124.

[8]   P.C. Marr and A.C. Marr, Ionic liquid gel materials: Applications in green and sustainable chemistry, *Green Chem.*, 18(2016), No. 1, p. 105.

[9]   F.K. Chong, F.T. Eljack, M. Atilhan, D.C.Y. Foo and N.G. Chemmangattuvalappil, Ionic liquid design for enhanced carbon dioxide capture-A computer aided molecular design approach, *Chem. Eng.*, 39(2014), No. 253.

[10] A.M. Vieira and A.E.C. Peres, The effect of amine type, pH, and size range in the flotation of quartz, *Miner. Eng.*, 20(2007), No. 10, p. 1008.

[11] A. Liu, J.C. Fan, and M.Q. Fan, Quantum chemical calculations and molecular dynamics simulations of amine collector adsorption on quartz (001) surface in the aqueous solution, *Int. J. Miner. Process.*, 134(2015), p. 1.

[12] V. Nunna, S.P. Suthers, M.I. Pownceby, and G.J. Sparrow, Beneficiation strategies for removal of silica and alumina from low-grade hematite–goethite iron ores, *Miner. Process. Extr. Metall. Rev.*, 43(2022), No. 8, p. 1049.

[13] D.S. He, K.X. Shang, W.M. Xie, F. Chen, M. Benzaazoua, and T.N. Aleksandrova, Study on the foam behavior of amine reagents adsorbed at gas–liquid and gas–liquid–solid interfaces, *Physicochem. Probl. Miner. Process.*, 57(2020), No. 1, p. 192.

[14] S.B. Liu, Y.Y. Ge, J. Fang, J. Yu, and Q. Gao, An investigation of froth stability in reverse flotation of collophane, *Miner. Eng.*, 155(2020), art. No. 106446.

[15] X.Q. Weng, G.J. Mei, T.T. Zhao, and Y. Zhu, Utilization of novel ester-containing quaternary ammonium surfactant as cationic collector for iron ore flotation, *Sep. Purif. Technol.*, 103(2013), p. 187.

[16] R.Q. Xie, Y.M. Zhu, J. Liu, and Y.J. Li, The flotation behavior and adsorption mechanism of a new cationic collector on the separation of spodumene from feldspar and quartz, *Sep. Purif. Technol.*, 264(2021), art. No. 118445.

[17] V.A. Araujo, N. Lima, A. Azevedo, L. Bicalho, and J. Rubio, Column reverse rougher flotation of iron bearing fine tailings assisted by HIC and a new cationic collector, *Miner. Eng.*, 156(2020), art. No. 106531.

[18] R. Li, C. Marion, E.R.L. Espiritu, R. Multani, X.Q. Sun, and K.E. Waters, Investigating the use of an ionic liquid for rare earth mineral flotation, *J. Rare Earths*, 39(2021), No. 7, p. 866.

[19] D. Azizi, F. Larachi, and M. Latifi, Ionic-liquid collectors for rare-earth minerals flotation:Case of tetrabutylammonium bis(2-ethylhexyl)-phosphate for monazite and bastnäsite recovery, *Colloids Surf. A*, 506(2016), p. 74.

[20] X.C. Zhu, H.B. Wei, M.Y. Hou, Q.B. Wang, X.F. You, and L. Li, Thermodynamic behavior and flotation kinetics of an ionic liquid microemulsion collector for coal flotation, *Fuel*, 262(2020), art. No. 116627.

[21] H. Qiu, C. Degenhardt, N. Feuge, D. Goldmann, and R. Wilhelm, Influencing the froth flotation of LiAlO$_2$ and melilite solid solution with ionic liquids, *RSC Adv.*, 12(2022), No. 45, p. 29562.

[22] H. Sahoo, S.S. Rath, and B. Das, Use of the ionic liquid-tri-caprylmethyl ammonium salicylate (TOMAS) as a flotation collector of quartz, *Sep. Purif. Technol.*, 136(2014), p. 66.

[23] H. Sahoo, S.S. Rath, S.K. Jena, B.K. Mishra, and B. Das, Aliquat-336 as a novel collector for quartz flotation, *Adv. Powder Technol.*, 26(2015), No. 2, p. 511.

[24] H. Sahoo, N. Sinha, S.S. Rath, and B. Das, Ionic liquids as novel quartz collectors: Insights from experiments and theory, *Chem. Eng. J.*, 273(2015), p. 46.

[25] H. Sahoo, S.S. Rath, B. Das, and B.K. Mishra, Flotation of quartz using ionic liquid collectors with different functional groups and varying chain lengths, *Miner. Eng.*, 95(2016), p. 107.

[26] H. Li, G. Mei, M. Yu, Q. Cheng, and G. Zhu, The mechanism study on aryl-substituted aromatic acid ionic liquid as the collector for quartz flotation, *Physicochem. Probl. Miner. Process.*, 55(2019), No. 5, p. 1239.

[27] J.Q. Zhou, G.J. Mei, M.M. Yu, and X.W. Song, Effect and mechanism of quaternary ammonium salt ionic liquid as a collector on desulfurization and desilication from artificial mixed bauxite using flotation, *Miner. Eng.*, 181(2022), art. No. 107523.

[28] Q.Z. Yuan, G.J. Mei, C. Liu, Q. Cheng, and S.Y. Yang, A novel sulfur-containing ionic liquid collector for the reverse flotation separation of pyrrhotite from magnetite, *Sep. Purif. Technol.*, 303(2022), art. No. 122189.

[29] Q. Cheng, G.J. Mei, W. Xu, and Q.Z. Yuan, Flotation of quartz using imidazole ionic liquid collectors with different counterions, *Miner. Eng.*, 180(2022), art. No. 107491.

[30] M. Wu, M.M. Yu, Q. Cheng, *et al.*, Flotation recovery of Y$_2$O$_3$ from waste phosphors using ionic liquids as collectors, *Chem. Phys. Lett.*, 825(2023), art. No. 140608.

[31] J. Fang, Y.Y. Ge, and J. Yu, Effects of particle size and wettability on froth stability in a collophane flotation system, *Powder Technol.*, 379(2021), p. 576.

[32] K.Y. Guo, T.F. Wang, G.Y. Yang, and J.F. Wang, Distinctly different bubble behaviors in a bubble column with pure liquids and alcohol solutions, *J. Chem. Technol. Biotechnol.*, 92(2017), No. 2, p. 432.

[33] S.R. Syeda, A. Afacan, and K.T. Chuang, Effect of surface tension gradient on froth stabilization and tray efficiency, *Chem.*

Eng. Res. Des., 82(2004), No. 6, p. 762.

[34] S. Andrew, Frothing in two-component liquid mixtures, [in] *Proceedings of the Symposium on Chemical Process Hazards with Special Reference to Plant Design*, United Kingdom, 1960, p. 73.

[35] G. Marrucci and L. Nicodemo, Coalescence of gas bubbles in aqueous solutions of inorganic electrolytes, *Chem. Eng. Sci.*, 22(1967), No. 9, p. 1257.

[36] P.C. Hiemenz and R. Rajagopalan, *Principles of Colloid and Surface Chemistry*, *Revised and Expanded*, CRC Press, Boca Raton, 2016.

[37] M.C. Fuerstenau and K.N. Han, *Principles of Mineral Processing*, SME media, Staines, 2003.

[38] L. Wang, Y. Peng, K. Runge, and D. Bradshaw, A review of entrainment: Mechanisms, contributing factors and modelling in flotation, *Miner. Eng.*, 70(2015), p. 77.

[39] X.Y. Zhu, H. Sun, D.J. Zhang, and C.B. Liu, Theoretical study on the interactions between methanol and imidazolium-based ionic liquids, *J. Mol. Model.*, 17(2011), No. 8, p. 1997.

[40] Y. Wang, H.R. Li, and S.J. Han, A theoretical investigation of the interactions between water molecules and ionic liquids, *J. Phys. Chem. B*, 110(2006), No. 48, p. 24646.

[41] J. Barthel, H. Krienke, and W. Kunz, *Physical Chemistry of Electrolyte Solutions*: *Modern Sspects*, Springer Science & Business Media, Berlin, 1998.

[42] H.L. Zhang, Z.J. Xu, W. Sun, *et al.*, Selective adsorption mechanism of dodecylamine on the hydrated surface of hematite and quartz, *Sep. Purif. Technol.*, 275(2021), art. No. 119137.

[43] S.R. Rao, *Surface Chemistry of Froth Flotation*: *Volume 1*: *Fundamentals*, Springer Science & Business Media, Berlin, 2013.

[44] V. Pino, C. Yao, and J.L. Anderson, Micellization and interfacial behavior of imidazolium-based ionic liquids in organic solvent–water mixtures, *J. Colloid Interface Sci.*, 333(2009), No. 2, p. 548.

[45] J.J. Wang, L.M. Zhang, H.Y. Wang, and C.Z. Wu, Aggregation behavior modulation of 1-dodecyl-3-methylimidazolium bromide by organic solvents in aqueous solution, *J. Phys. Chem. B*, 115(2011), No. 17, p. 4955.

[46] A. Rodríguez, M.D. Graciani, and M.L. Moyá, Effects of addition of polar organic solvents on micellization, *Langmuir*, 24(2008), No. 22, p. 12785.